

# Dynamics of Self-Adjusting Systems with Noise

Paul Melby\*, Nicholas Weber, and Alfred Hübler

*Center for Complex Systems Research, Department of Physics,  
University of Illinois at Urbana-Champaign, 1110 West Green Street, Urbana, Illinois, 61801\**

We perform studies of several self-adjusting systems with noise. In our analytical and numerical studies, we find that the dynamics of the self-adjusting parameter can be accurately described with a rescaled diffusion equation. We find that adaptation to the edge of chaos, a feature previously ascribed to self-adjusting systems, is only a long-lived transient when noise is present in the system. In addition, using analytical, numerical, and experimental studies, we find that noise can cause chaotic outbreaks where the parameter reenters the chaotic regime and the system dynamics become chaotic. We find that these chaotic outbreaks have a power law distribution in length.

PACS numbers: 05.65.+b, 05.45.Pq, 05.45.Gg, 05.40.-a

## I. INTRODUCTION

We study a specific type of adaptive systems, known as self-adjusting systems [1]. Self-adjusting systems have the characteristic that the parameters of the system are slowly varying, rather than constant. The dynamics of these parameters are governed by a low-pass filtered feedback from the dynamical variables of the system. In recent numerical and experimental studies, self-adjusting systems have been found to adapt to the edge of chaos [2] and that this adaptation is robust with respect to an external controlling force [3]. In self-adjusting vibrating strings [4] and soap films [5], it has been found that resonances are attractive. In addition, models of coupled neurons with self-adjusting coupling strengths have been found to exhibit robust synchronization [6] and suppression of chaos [7].

The parameters in a self-adjusting system have a simple, overdamped motion without attractor. They are distinguished from the dynamical variables through a separation of time scales [8], that is, they change much more slowly than the dynamical variables. The parameters dynamics are governed by a low-pass filtered feedback with DC cutoff from the dynamical variables of the system itself. Previous numerical results for the self-adjusting logistic map were consistent with the parameter changing in a random fashion until it reaches the edge of chaos [2]. This process, called adaptation to the edge of chaos, is observed when parameter values show a high probability of asymptotically reaching a value in which a small perturbation in the parameter value changes the resulting dynamics from chaotic to non-chaotic, or vice-versa. In Sec. II of this paper we introduce the self-adjusting Bernoulli shift map with noise and study this map both numerically and analytically. Motivated by the idea that the parameter's dynamics are random, we describe the probability distribution of parameters with a scaled diffu-

sion equation and find good agreement with the simulations. We show that the parameter adapts to the edge of chaos on short time scales and is driven further from the chaotic regime on longer time scales as a result of noise in the system. In Sec. III we further extend this diffusion equation approach to describe chaotic outbreaks in the system, where the parameter reenters the chaotic regime, also under the influence of noise, and the system dynamics become chaotic. We find that the probability distribution of the duration of outbreaks obeys a power-law. Numerical simulations of a self-adjusting logistic map and experimental results from a self-adjusting Chua's circuit agree with the power-law distribution in outbreaks. In Sec. IV, we summarize our results and discuss the application of low-pass filtered feedback as a method for controlling chaos.

## II. SELF-ADJUSTING BERNOULLI SHIFT MAP

If  $x_t$  is the dynamical variable,  $\eta_t$  is a very small noise term,  $a_t$  is the self-adjusting parameter,  $t$  is time,  $f_t$  is a low-pass filtered feedback of the  $x_t$  dynamics with DC cutoff, and  $\epsilon$  is a small number, then the self-adjusting Bernoulli shift map with noise is given by:

$$\begin{aligned} x_{t+1} &= a_t x_t + \eta_t \quad \text{mod } 1 & 0 \leq x_t < 1 \\ a_{t+1} &= a_t + \epsilon f_t(x) & 0 \leq a_t \leq 2 \end{aligned} \quad (1)$$

For the traditional Bernoulli shift map,  $a_t = a = 2$  and  $\eta_t = 0$ . The value of  $a$  determines the type of dynamics which occurs for the dynamical variable,  $x_n$ . Disregarding noise, if  $0 < a < 1$ , then the dynamics of  $x_n$  is exponential decay with a stable fixed-point attractor at  $x = 0$ . For  $a = 1$ , the map is equivalent to the identity map and the dynamics are constant. For  $1 < a \leq 2$  the dynamics are chaotic [9]. Because  $a = 1$  is the transition from stationary behavior in  $x$  to chaotic behavior in  $x$ , it is referred to as the edge of chaos. In the perturbed Bernoulli shift map, the dynamics are much the same. For  $0 < a < 1$ , the dynamics are noisy fluctuations near 0. For the same noise sequence, nearby

---

\*Present address: Department of Physics, Georgetown University, 37th and O Streets NW, Washington, DC 20057

trajectories will converge exponentially. For  $a = 1$  the dynamics become a random walk. However, the mod function will tend to separate nearby trajectories. For  $1 < a \leq 2$ , the dynamics remain chaotic even in the presence of noise, with exponential separation of nearby trajectories. Therefore,  $a = 1$  remains the edge of chaos in the perturbed Bernoulli shift map. Because of the separation of timescales between the  $x_t$  and  $a_t$ ,  $a = 1$  is also the edge of chaos in the self-adjusting Bernoulli shift.

To study the dynamics of the system, a low-pass filter must be chosen for the feedback term in equation 1. The same filter used in the previous studies of the logistic map [2] is employed. This filter can be calculated in the numerical simulations with a Fourier analysis of the time series for  $x_n$ . If  $N$  time steps are used, the Fourier sine and cosine coefficients are given by:  $c_{tk} = (2/N) \sum_{\tau=0}^{N-1} x(\tau+t-N+1) \sin(2\pi k\tau/N)$ ,  $d_{t0} = (1/N) \sum_{\tau=0}^{N-1} x(\tau+t-N+1)$ , and  $d_{tk} = (2/N) \sum_{\tau=0}^{N-1} x(\tau+t-N+1) \cos(2\pi k\tau/N)$  for  $k = 1, 2, \dots, (N-1)/2$  where  $k$  is the frequency. If  $N$  is odd, an extra term is needed:  $d_{t\frac{N+1}{2}} = (1/N) \sum_{\tau=0}^{N-1} x(\tau+t-N+1) \cos(\pi(N+1)t/N)$ .

To make a low-pass filter with a very low cutoff frequency and DC cutoff, only the terms  $c_{n1}$  and  $d_{n1}$  would be kept. The back transformation would then become:

$$\bar{x}_t = c_{t1} \sin\left(\frac{2\pi t}{N}\right) + d_{t1} \cos\left(\frac{2\pi t}{N}\right) \quad (2)$$

If the forcing is only applied once every  $N$  steps, and is evaluated when  $n$  is a multiple of  $N$ ,  $f_n$  becomes simply:

$$f_t = \begin{cases} \epsilon \bar{x}_N = \epsilon d_{t1} & \text{if } t = iN \\ 0 & \text{if } t \neq iN \end{cases} \quad i = 1, 2, 3, \dots \quad (3)$$

Numerical simulations of the self-adjusting Bernoulli-shift were performed with different noise levels. The results for zero noise agree with those found in the self-adjusting logistic map [2]. If the probability distribution of parameter values initially flat and its asymptotic distribution is found, the system asymptotically approaches a distribution with a very large peak at the edge of chaos,  $a = 1$ , as shown in Fig 1. Therefore, we say that the system exhibits adaptation to the edge of chaos.

Both with and without noise, the feedback term was analyzed and found to be  $\delta$ -correlated and Gaussian distributed, with standard deviation,  $\sigma$ , a function of  $a$ . These properties of the feedback serve to motivate a description of the evolution of the parameter as a random walk, or diffusive process. The diffusion constant,  $D$ , of the parameter's dynamics can be found from the standard deviation,  $\sigma$ , of the feedback with the relation  $D = \sigma^2/2$  [10]. In order to describe the adaptation process, a statistical approach is taken. If  $P(a, t)$  is the probability of finding the parameter at a value of  $a$  at time  $t$ , then we can describe the parameter dynamics with a diffusion equation:

$$\frac{dP}{dt} \simeq \begin{cases} D_p \frac{d^2 P}{da^2} & 0 < a < 1 \\ D_c \frac{d^2 P}{da^2} & 1 < a < 2 \end{cases} \quad (4)$$

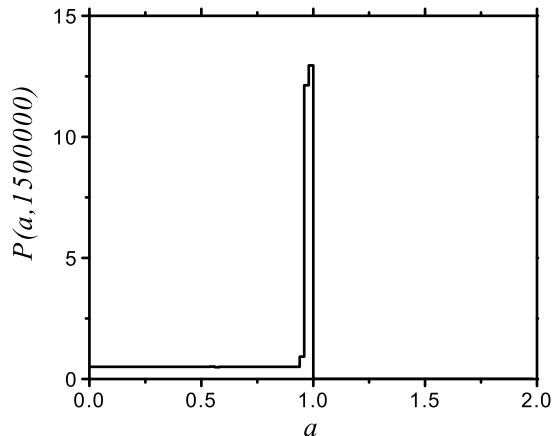


FIG. 1: Adaptation to the edge of chaos. The probability,  $P$  of finding the parameter,  $a$  at a given value at time,  $t = 1.5 \times 10^6$ . The initial probability distribution is flat across the entire parameter range,  $P(a, 0) = 0.5$ . The probability distribution shows a large peak at the edge of chaos,  $a = 1$ . The numerical simulations used 5000 separate trajectories for  $a$ , with  $\epsilon = 0.1$ ,  $N = 10$ , and noise,  $\eta$  with standard deviation  $\sigma_\eta = 0$ .

where  $a$  is the parameter,  $D$  are the diffusion constants, with  $D_c > D_p$  and  $a = 1$  is the edge of chaos. As an approximation, the diffusion constant is split into two separate diffusion constants, one for the chaotic regime,  $D_c$  and one for the non-chaotic regime,  $D_p$ . This, however, is an approximation, as  $\sigma^2$  has a more complicated dependence on  $a$ . This approximation is discussed in more detail later in the paper. In order to solve Eq. 4 analytically, the probabilities can be scaled by the diffusion constants so that a single diffusion constant can be used. If  $D_p$  is chosen as the diffusion constant for the scaled probabilities, the probabilities can be written as:

$$P_s(a_s, t) = \begin{cases} P(a_s, t) & 0 < a_s < 1 \\ P(a_s, t) \frac{D_c}{D_p} & 1 < a_s < 2\theta \end{cases} \quad (5)$$

where  $P_s$  is the scaled probability,  $P(a_s, t)$  is the probability of finding the scaled parameter at value  $a_s$  at time  $t$ ,  $D_c$  is the diffusion constant at parameter values leading to chaotic  $x$  dynamics,  $D_p$  is the diffusion constant at parameter values leading to fixed point  $x$  dynamics, and  $\theta = 0.5(1 + \frac{D_p}{D_c})$ . In addition to the probabilities, the parameter has also been scaled:

$$a_s = \begin{cases} a & 0 < a < 1 \\ 1 + \frac{D_p}{D_c}(a - 1) & 1 < a < 2 \end{cases} \quad (6)$$

In this way, the total probability in the system remains 1. This scaling of the probability,  $P$ , and the parameter,  $a$ , leads to a scaled diffusion equation:

$$\frac{dP_s}{dt} = D_p \frac{d^2 P_s}{da_s^2} \quad (7)$$

where  $P_s$  is the scaled probability,  $a_s$  is the scaled parameter, and  $D_p$  is the diffusion constant in the non-chaotic regime. This equation can be solved analytically to find a time-dependent solution for the scaled probability distribution,  $P_s(a, t)$ .

To describe the adaptation process, we use an initial condition  $P(a) = \text{constant}$  with reflecting boundaries at  $a = 0$  and  $a = 2$ . When scaled, this initial condition becomes:

$$P_s(a_s, 0) = \begin{cases} 0.5 & 0 < a_s < 1 \\ 0.5 \frac{D_c}{D_p} & 1 < a_s < 2\theta \end{cases} \quad (8)$$

where 0.5 is the initial unscaled probability and  $\theta = 0.5(1 + \frac{D_p}{D_c})$ .

To get the time dependent solution, we use Fourier series, with an even periodic (cosine) expansion. Using this even expansion properly accounts for the reflecting walls at  $a = 0$  and  $a = 2\theta$ . The cosine expansion is given by:

$$\alpha_0 = \frac{1}{4} \int_0^{2\theta} P_s(a_s, 0) da_s \quad (9)$$

$$\alpha_n = \frac{1}{2} \int_0^{2\theta} P_s(a_s, 0) \cos\left(\frac{n\pi a_s}{2\theta}\right) da_s \quad (10)$$

with  $\alpha_n$  as the cosine coefficient for frequency  $n$ . The back transformation is given by:

$$P_s(a_s, 0) = \alpha_0 + \sum_{n=1}^{\infty} \alpha_n \cos\left(\frac{n\pi a_s}{2\theta}\right) \quad (11)$$

By using the initial conditions from equation 8 in the Fourier expansion, equations 9 and 10, we get the following cosine coefficients:

$$\alpha_0 = \frac{1}{4\theta} \left(1 + \frac{D_p}{D_c}\right) \quad (12)$$

$$\alpha_n = \frac{1}{n\pi} \left(1 - \frac{D_c}{D_p}\right) \sin\left(\frac{n\pi}{2\theta}\right) \quad (13)$$

where  $\alpha_n$  is the cosine coefficient for frequency  $n$ ,  $D_p$  and  $D_c$  are the diffusion constants in the non-chaotic and chaotic regimes, respectively, and  $\theta = 0.5(1 + \frac{D_p}{D_c})$ .

By using the Fourier series expansion, we can write the solution to the diffusion equation in terms of the Fourier coefficients:

$$P_s(a_s, t) = \alpha_0 + \sum_{n=1}^{\infty} \alpha_n \cos\left(\frac{n\pi a_s}{4}\right) e^{-n^2 \pi^2 D_p t / 16} \quad (14)$$

where  $D_p$  is the diffusion constant in the non-chaotic regime. Once  $P_s(a_s, t)$  is calculated, it is a simple scaling from Eq. 5 to find  $P(a, t)$ :

$$P(a, t) = \begin{cases} P_s(a, t) & 0 < a < 1 \\ P_s(1 + \frac{D_p}{D_c}(a-1), t) \frac{D_p}{D_c} & 1 < a < 2 \end{cases} \quad (15)$$

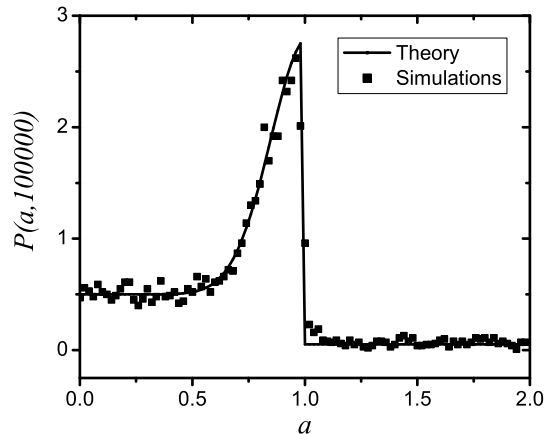


FIG. 2: Probability distribution for a  $t = 1 \times 10^5$ . The peak near the edge of chaos is now shorter and wider. The parameter values are moving further into the nonchaotic regime. The numerical simulations use the same parameters as Fig. 1, but with  $\eta$  having standard deviation  $\sigma_\eta = 0.1$ . The theoretical calculations used 50,000 cosine coefficients, and  $D_p = 1.786 \times 10^{-6}$ ,  $D_c = 9.508 \times 10^{-5}$ , as measured from the numerical simulations.

Fig. 2 shows  $P(a, t)$  for both the numerical simulations as well as for the theoretical result for  $t = 100000$ . As can be seen in the figure, there is a peak in the probability distribution at the edge of chaos,  $a = 1$ . The analytical result uses the diffusion constants,  $D_p$  and  $D_c$ , found from the numerical simulations. Therefore, there are no free parameters in the analytical curve. The overall agreement between the simulations and the theory is quite good. The width of the peak for the system with noise is much wider than in the case with no noise, shown in Fig. 1, where the width of the peak is from the binning of the data. Therefore, we can conclude that noise in the system is causing the peak at the edge of chaos to broaden into the nonchaotic regime. When looking at the properties of the feedback, the role of noise becomes obvious. For  $a < 1$ , the feedback is 0 when there is no noise in the system, while it is small, but positive for systems with noise. While a large peak at the edge of chaos shows up initially, it is only a transient in the system. Therefore, we can say that in self-adjusting systems with noise, adaptation to the edge of chaos is only a long-lived transient.

The asymptotic distribution can be calculated explicitly, as the scaled probability distribution,  $P_s(a, \infty)$  would asymptotically become flat. This asymptotic distribution is  $P_s(a, \infty) = \alpha_0$ , the zeroth cosine component, calculated in Eq. 12. Returning this back to the unscaled distribution,  $P(a, \infty)$ , gives:

$$P(a, \infty) = \begin{cases} \alpha_0 & 0 < a < 1 \\ \frac{\alpha_0 D_p}{D_c} & 1 < a < 2 \end{cases} \quad (16)$$

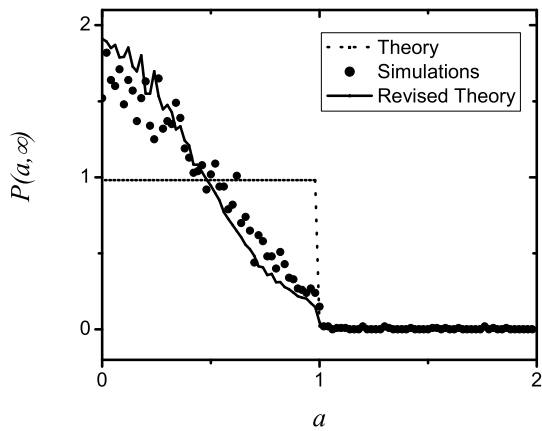


FIG. 3: Asymptotic probability distribution,  $P(a, \infty)$  as a function of the parameter,  $a$ . Shown are the numerical simulations, which shows  $P(a, 5 \times 10^6)$ , 5000 separate trajectories for  $a$ , with  $\epsilon = 0.1$ ,  $N = 10$ , and noise,  $\eta$  with standard deviation  $\sigma_\eta = 0.1$ . The first set of theoretical calculations used  $D_p = 1.786 \times 10^{-6}$  and  $D_c = 9.508 \times 10^{-5}$ , as measured from the numerical simulations. The revised theoretical calculations use the full  $a$  dependent diffusion constant,  $D_a$ , measured in the numerical simulations. For the numerical results, we approximate  $P(a, \infty)$  with  $P(a, 1 \times 10^7)$ .

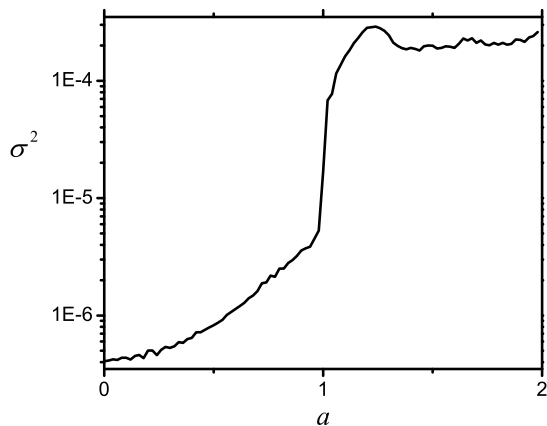


FIG. 4: Variance,  $\sigma^2$ , of the feedback  $f$  as a function of the parameter,  $a$ . In these simulations,  $N = 10$ ,  $\epsilon = 0.1$ , and the noise,  $\eta$  has standard deviation  $\sigma_\eta = 0.1$ .

where  $a$  is the parameter,  $D_p$  and  $D_c$  are the diffusion constants in the non-chaotic and chaotic regimes and  $\alpha_0$  is the zeroth cosine coefficient, calculated in equation 12. This distribution leads to a very low probability of finding the parameter in the chaotic regime. Therefore, the self-adjusting Bernoulli Shift is said to suppress chaos. The results of this calculation, as well as for the numerical simulations can be seen in Fig. 3. The calculation from Eq. 16, however, does not show good agreement

with the numerical simulations. The likely cause is the approximation that the diffusion constant in the non-chaotic regime,  $D_p$  is constant. It is not, as shown in Fig. 4. The standard deviation in the chaotic regime is nearly constant, with a small peak in the chaotic regime near the edge of chaos, at  $a = 1$ . Near the edge of chaos, there is critical slowing down of the  $x$  dynamics [11]. Because of this, there exists a large low-frequency component to the  $x$  dynamics, and hence the low-pass filtered feedback,  $f$  has larger values for  $a$  close to 1 than for other values. However, the feedback is still an order of magnitude larger for all  $a > 1$  than for any  $a < 1$ , showing that the “dynamical noise” of the chaotic dynamics is much larger than the noise added to the system. The fact that the variance of the feedback,  $\sigma^2$  is not constant in the non-chaotic regime is lacking in the scaled diffusion equation, Eq. 7. This approximation causes errors in the probability distribution,  $P(a, t)$ , for longer time scales, when the parameter begins to explore more of the non-chaotic regime.

A better solution for the asymptotic distribution can be found using the feedback as a function of  $a$ . The probability is found by scaling the flat scaled probability by  $1/D$ , so the asymptotic probability distribution,  $P(a, \infty)$ , would be proportional to  $1/D$ :

$$P(a, \infty) \propto \frac{\alpha_0 D(0)}{D(a)} \quad (17)$$

where  $D(a)$  is the diffusion constant as a function of  $a$  and  $D(0)$  is the diffusion constant for  $a = 0$ . This calculation, properly normalized, is also included in Fig. 3 and shows much better agreement with the numerical simulations.

### III. CHAOTIC OUTBREAKS

While chaos is suppressed in self-adjusting systems, there is still a small probability of finding the parameter in the chaotic regime. From the perspective of a single trajectory of the parameter, it will spend most of its time in the nonchaotic regime and make occasional trips into the chaotic regime. These are called chaotic outbreaks and we wish to understand the properties of these outbreaks, namely the distribution of outbreaks as a function of duration,  $L$ . To do this, we look at the self-adjusting logistic map, given by:

$$\begin{aligned} x_{n+1} &= a_n x_n (1 - x_n) + \eta_n & 0 \leq x_n \leq 1 \\ a_{n+1} &= a_n + \epsilon f_n(x) & 0 \leq a_n \leq 4 \end{aligned} \quad (18)$$

where  $x_n$  is the dynamical variable,  $\eta_n$  is a very small noise term,  $a_n$  is the self-adjusting parameter,  $n$  is time,  $f_n$  is a low-pass filtered feedback of the  $x_n$  dynamics,  $x$ .  $\epsilon$  is a small number. The dynamics for both the standard logistic map, where  $a = \text{constant}$ , and the self-adjusting logistic map are summarized in Ref. [2]. It is important to note, however, that the edge of chaos in the logistic map with a very small noise level remains at  $a = 3.56$ .

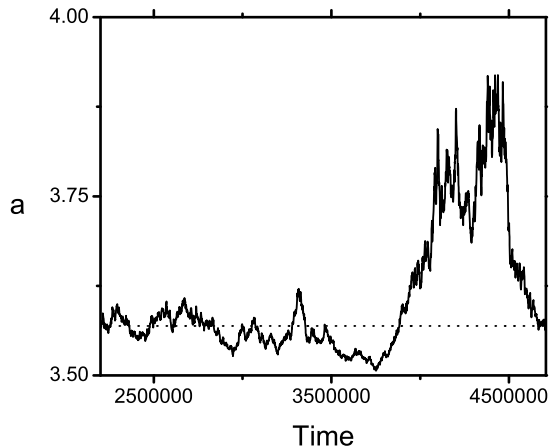


FIG. 5: Chaotic outbreaks in the self-adjusting logistic map. The dotted line shows the edge of chaos. The parameter enters and leaves the chaotic regime several times in this plot, with each trip considered a chaotic outbreak. There exists an outbreak of very long duration in the right-hand side of the plot. The parameters in this simulation were  $N = 20$ ,  $\epsilon = 0.01$ , and  $\sigma_\eta = 0.01$ .

The low-pass filter used in the system is the same as the filter as described in Sec. II. Because there is noise in the system, the feedback when the parameter leads to periodic dynamics will be nonzero. This means that if the parameter is near to the edge of chaos, it may diffuse back into the chaotic regime. After it has reached the chaotic regime, it will perform a random walk until it returns. This is shown in Figure 5. In this figure, the parameter hovers near the edge of chaos, and then enters the chaotic regime, where it spends some time before returning. Several long time outbreaks are shown in the figure, as well as several very short outbreaks.

### A. Diffusion Equation

We again model this process using a diffusion equation. Once again, we will use a Fourier expansion to find the solution to the diffusion equation. Assuming that the parameter starts a small distance in the chaotic regime, up to  $\delta a$ , we use the initial conditions:

$$P(a, 0) = \begin{cases} 0 & a = 0 \\ 1/\Delta a & 0 < a < \Delta a \\ 0 & a > \Delta a \end{cases} \quad (19)$$

Where  $a$  is the distance of the parameter from the edge of chaos and  $\Delta a$  is the distance into the chaotic regime that the parameter starts. We also treat the wall at  $a = 0$  as an absorbing wall, which can be done by using an odd

half-range fourier expansion:

$$\beta(k) = \frac{2}{\pi} \int_0^\infty P(a, 0) \sin(ka) da \quad (20)$$

with  $\beta(k)$  being the sine coefficient for frequency  $k$ . The back transformation is:

$$P(a, 0) = \int_0^\infty \beta(k) \sin(ka) dk \quad (21)$$

By performing the sine expansion, we get the following coefficients:

$$\beta(k) = \frac{4}{\Delta a \pi k} \sin^2\left(\frac{k \Delta a}{2}\right) \quad (22)$$

The time dependent solution to the diffusion equation is written in terms of the Fourier components:

$$P(a, t) = \int_0^\infty \beta_k \sin(ka) e^{-k^2 D_c t} \quad (23)$$

Because of the absorbing boundary, the value of  $P$  will be decreasing with time. However, what we are interested in is finding the probability of an outbreak of time  $T$ ,  $p(T)$ . This corresponds to the rate of change of the total probability distribution evaluated at time  $T$ :

$$p(T) = \left. \frac{dP(t)}{dt} \right|_{t=T} \quad (24)$$

where  $P(t)$  is the probability of finding the parameter at any positive value of  $a$ . However, by taking this derivative first, before finding the total probability, the math is simplified. Taking the derivative gives of  $P(a, t)$  from equation 23 gives:

$$p(a, T) = -D_c \int_0^\infty \beta(k) k^2 \sin(ka) e^{-k^2 D_c T} dk \quad (25)$$

Plugging in the values of  $\beta_k$  leads to:

$$p(a, T) = -\frac{4D_c}{\Delta a \pi} \int_0^\infty \sin^2\left(\frac{k \Delta a}{2}\right) k \sin(ka) e^{-k^2 D_c T} dk \quad (26)$$

Performing the integral leads to:

$$p(a, T) = \frac{D_c}{4\sqrt{\pi}\Delta a(D_c T)^{\frac{3}{2}}} \left( \Delta a \left( 1 - a e^{\frac{a \Delta a}{D_c T}} \right) + a \left( 1 + e^{\frac{a \Delta a}{D_c T}} - 2e^{\frac{\Delta a(2a + \Delta a)}{4D_c T}} \right) \right) \quad (27)$$

This equation still needs to be integrated over  $a$ , so that we have the rate of change of the total probability. Integrating over  $a$  from 0 to  $\infty$ , we get the following expression for  $p(T)$ :

$$p(T) = \frac{D_c e^{-\frac{\Delta a^2}{4D_c T}} - D_c}{\Delta a \sqrt{\pi D_c T}} \quad (28)$$

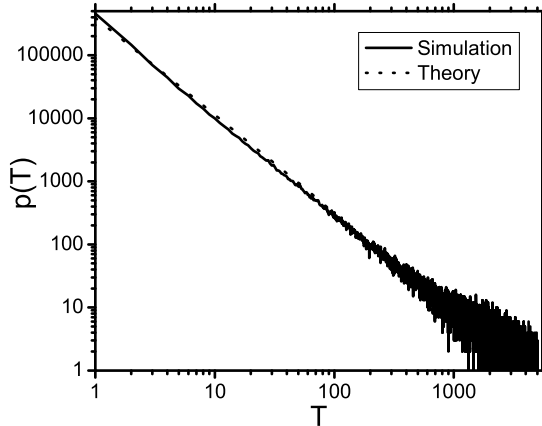


FIG. 6: Probability distribution,  $p(T)$  of the chaotic outbreaks for  $\epsilon = 0.01$ . The dependence on the length of the outbreak is approximately a power law with exponent -1.5

Because  $\Delta a$  is very small, we can approximate the exponential with a series expansion, to order  $\Delta a^2$ :

$$p(T) = \frac{\Delta a}{4\sqrt{\pi D_c}} T^{-\frac{3}{2}} \quad (29)$$

This expression for  $p(T)$  yields a power law dependence on  $T$  with exponent -1.5. It should be noted that this equation is related to the Inverse Gaussian function [12], which arises in first passage time problems. In essence, we are really looking for the first passage time distribution of the parameter passing back into the periodic regime. Therefore, the -1.5 power law is easily understood. In Figure 6, the probability distribution from Eq. 29 and numerical simulations are shown. As can be seen, the distribution of the outbreaks approximates a power-law over several orders of magnitude. The exponent of the approximate power-law is -1.5, showing that the description of the parameter's dynamics as a diffusion process accurately describes what is seen in the self-adjusting system.

### B. Chaotic Outbreaks in the Self-Adjusting Chua Circuit

Experimental verification of adaptation to the edge of chaos in self-adjusting systems has been shown in a self-adjusting Chua oscillator [3, 13]. We have used the same experimental setup to look at the presence of chaotic outbreaks in the self-adjusting Chua circuit. Because of the unavoidable noise in the experimental system, no additional noise needs to be added to cause a chaotic outbreak. A circuit diagram of the Chua circuit is shown in Fig 7. The two key elements to the circuit are the nonlinear resistor, described elsewhere [13, 14] and the variable resistor [13]. In the self-adjusting Chua Oscillator, the

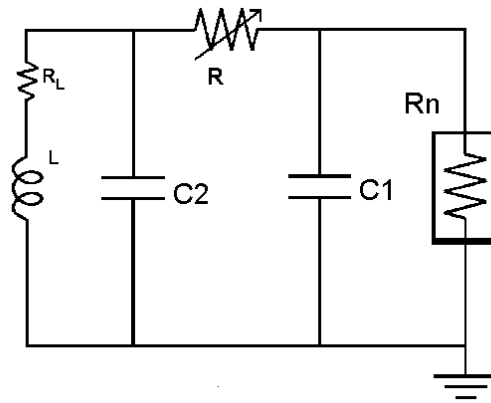


FIG. 7: Circuit diagram for the Chua circuit.  $N_R$  is a nonlinear resistor. In our experimental circuit,  $L = 91.9$  mH,  $R_L = 17.3\Omega$ ,  $C_1 = 52.31$  nF,  $C_2 = 567$  nF, and  $R$  varies from  $1350\Omega$  to  $1950\Omega$ . Reproduced from Weber, 2001.

variable resistor is changed through a low-pass filtered feedback from the dynamical variable, in this case the voltage  $V_{C1}$  across the capacitor,  $C_1$ :

$$R_{t+1} = R_t + \epsilon L(V_{C1}) \quad (30)$$

where  $R$  is the variable resistor,  $\epsilon$  is a scaling factor, and  $L$  is a low pass filter on the  $V_{C1}$  dynamics. To implement the filter, we take a window of length  $N$  and then measure the voltage,  $V_{C1}$ , at equally spaced intervals in the window. This time series for  $V_{C1}$  is weighted by a Hanning window [15]. At this point, the filter is implemented in the same fashion as described for the Bernoulli shift map, above. The key difference is the weighting, which becomes more important when taking discrete experimental data from a continuous time process.

The dynamics of the Chua circuit, including the resistance dependence of the oscillations are described in Refs. [13, 14]. The important aspect here is that, at a value of  $R = 1400\Omega$  is the transition from a large limit cycle dynamics to a double-scroll chaotic dynamics. This point, then, represents the edge of chaos. To study the outbreaks in the Chua circuit, we set the initial value of the resistance to  $R = 1400$ . Then, we observe the parameter make a chaotic outbreak ( $R > 1400$ ) and count the length of time that it spends in the chaotic regime. We show the distribution of outbreaks of duration,  $T$  in Fig. 8. It is clear that the distribution follows the same -1.5 power law as derived for the logistic map, above. This is, again, what is to be expected from a diffusive process. At short times, there is a disagreement with the power-law. This comes about, in the experimental setup, because of a hysteresis effect in the circuit.

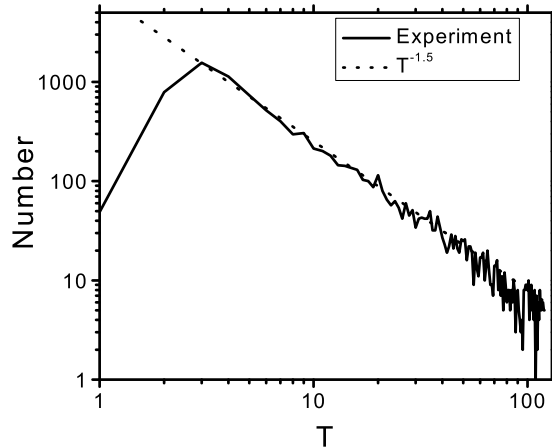


FIG. 8: Probability distribution of chaotic outbreaks for the self-adjusting Chua circuit. The experimental distribution is approximately a  $-1.5$  power law.

#### IV. CONCLUSIONS

We have studied the self-adjusting Bernoulli-Shift map, both with numerical simulations and analytical calculations. We have found that, on short time scales, this map exhibits adaptation to the edge of chaos, as did the self-adjusting logistic map [2, 3]. However, noise in the system destroys the initial peak in the probability distribution at the edge of chaos, and the characteristic feature of the resulting distribution is that it has a low probability of being found in the chaotic regime. Therefore, we

say that the system suppresses chaos. These results were found using both a scaled diffusion equation approach, as well as numerical simulations.

We have also shown that, for the self-adjusting logistic map with noise, that after the parameter has evolved to the edge of chaos it may re-enter the chaotic regime. We have called this process a chaotic outbreaks. We have shown that the probability distribution of the length of the chaotic outbreaks can also be described with a diffusion equation, which results in a power law distribution. We find that our analytical expressions show good agreement with numerical simulations. In addition, we find that in an experimental system, the same power-law behavior is observed.

Both of these results are important to applications of low-pass filtered feedback as a method of controlling chaos. The control of chaos has been an area of intense interest since the initial work in the field [16, 17]. Low-pass filtered feedback from the dynamical variables to the parameters of a system provides an easy way to suppress chaos in the system. No knowledge of the systems dynamics are necessary, and the suppression of chaos is robust against linear controlling forces [3]. However, the presence of noise leads to the undesirable possibility of chaotic outbreaks. Therefore the usefulness of this as a control method in real-world systems may be somewhat limited.

#### Acknowledgments

This research was supported by the National Science Foundation Grant no. NSF PHY 01-40179

- 
- [1] T. Ritz, A.W. Hübler, in *Proceedings of the 1996 International Workshop on Control Mechanisms for Complex Systems*, (Las Cruces, NM, December 1996), pp. 63-65.
  - [2] P. Melby, J. Kaidel, N. Weber, and A. Hübler, *Phys. Rev. Lett.* **84**, 5991 (2000).
  - [3] P. Melby, N. Weber, and A. Hübler, *Fluct. Noise Lett.* **2**, L285 (2002).
  - [4] A. Boudaoud, Y. Couder, and M. Ben Amar, *Euro. Phys. J. B* **9**, 159 (1999).
  - [5] A. Boudaoud, Y. Couder, and M. Ben Amar, *Phys. Rev. Lett.* **82**, 3847 (1999).
  - [6] V.P. Zhigulin, M.I. Rabinovich, R. Huerta, and H.D.I. Abarbanel, *Phys. Rev. E* **67** 021901 (2003).
  - [7] V.P. Zhigulin, M.I. Rabinovich, Abstract J1.028 in March Meeting 2003 Scientific Program, Bulletin of the American Physical Society (unpublished), available online at: <http://www.eps.org/aps/meet/MAR03/baps/abs/S3210028.html>
  - [8] H. Haken, *Synergetics* (Springer, Berlin, 1978), pp. 191-223.
  - [9] H.G. Schuster *Deterministic Chaos* (Physik-Verlag, Weinheim, 1988), pp. 21-23.
  - [10] H. Haken, *Synergetics* (Springer, Berlin, 1978), pp. 75-78.
  - [11] H.G. Schuster *Deterministic Chaos* (Physik-Verlag, Weinheim, 1988), p. 28.
  - [12] V. Seshadri, *The inverse Gaussian distribution: Statistical theory and applications*, (Springer-Verlag, New York, 1999).
  - [13] N. Weber, *Modelling and Control of Evolving Noisy Chaotic Systems* Ph.D. Dissertation, Dept. of Physics University of Illinois (2001).
  - [14] L.O. Chua, T. Matsumoto, and M. Komuro, *IEEE Trans. on Circuits and Systems* **cas-33** (1986).
  - [15] E. C. Ifeachor and B. W. Jervis, *Digital signal processing. A practical approach* (Addison-Wesley, Reading, MA, 1993).
  - [16] A. Hübler, *Helv. Phys. Acta* **62** 343 (1989).
  - [17] E. Ott, C. Grebogi, J. Yorke, *Phys. Rev. Lett.* **64** 1196 (1990).